DEVELOPMENT AND ASSESSMENT OF POLYMERIC NANOPARTICLE-BASED CAPSULE COMPOSITES FOR PEPTIC **ULCER TREATMENT**

Mr. Sahil B. Shaikh^{1*}, Dr. Sunil J. Aher², Dr. Kumudini R. Pawar³, Mr. Saurabh Nimesh⁴, Disha Arora⁵, Niraysinh M. Rathod⁶, Kartik Adake⁷

¹Department of Pharmaceutics, VJSM'S Institute of Pharmacy, Ale, 54G6+R58, Maharashtra, 412411.

²Department of Pharmaceutics, SERS's Sanjivani College of Pharmaceutical Education & Research, Kopargaon, Maharashtra, 423603.

³Department of Pharmaceutical Chemistry, Abhinav Education Society's College of Pharmacy, Narhe, Pune, Maharashtra, 411041.

⁴Department of Pharmacology, Metro College of Health Sciences & Research, Greater Noida, Uttar Pradesh, 201310.

⁵Faculty of Pharmaceutical Sciences, The ICFAI University, Baddi, Himachal Pradesh ⁶Department of Pharmaceutics, Tathya Pharmacy College, NH-48, Nr. R. N. Desai Petrol Pump, Chikhli, Gujarat, 396521.

⁷Department of zoology, St. Xavier's College (Empowered Autonomous Institute), Mumbai, Maharashtra, 400001.

Corresponding Author-Mr. Sahil Bashir Shaikh.

Email-shaikhsahil26586@gmail.com

VJSM'S Institute of Pharmacy, Ale, 54G6+R58, Maharashtra 412411.

KEYWORDS ABSTRACT

Nanoparticles,

NDDS, Polymeric The study focused on the formulation and evaluation of polymeric nanoparticle capsule composites, using a combination of natural polymer chitosan and synthetic

Peptic Ulcer, Anti-polymer methylcellulose, to improve drug delivery systems. These polymers were Ulcerating Agent,

chosen for their biocompatibility and ability to enhance drug stability and release. Among various formulations tested, formulation F2 emerged as the most optimized, demonstrating excellent performance across key parameters. F2 displayed the smallest particle size (78.04 nm), which enhances cellular uptake and increases the surface area available for drug interaction. The formulation also showed the highest entrapment efficiency (97.93%) and excellent drug content (98.84%), ensuring a high payload and effective drug delivery. The strong zeta potential (53.4 mV) further confirmed the formulation's stability, minimizing aggregation and enhancing dispersion in biological systems. In vitro drug release studies showed that F2 had a remarkable release rate of 98.45% over 6 hours, outperforming all other formulations. This rapid drug release is beneficial for medications requiring fast absorption or quick therapeutic effects. Additionally, when compared to traditional lansoprazole capsules, F2 showed superior drug release, suggesting potential for better therapeutic outcomes. Animal studies also supported F2's efficacy, as it effectively treated stomach inflammation and ulcerative conditions, showing superior therapeutic performance compared to other formulations. These results indicate that F2 is a promising candidate for clinical applications in treating gastric disorders, offering enhanced drug delivery, optimized release characteristics, and improved therapeutic effects, making it an ideal choice for future use.



INTRODUCTION-

Peptic ulcer disease (PUD) is a common gastrointestinal disorder characterized by the formation of ulcers in the stomach or duodenum due to factors such as Helicobacter pylori infection, excessive gastric acid secretion, and prolonged use of nonsteroidal anti-inflammatory drugs (NSAIDs) [01]. Conventional treatments primarily involve the use of proton pump inhibitors (PPIs), H2-receptor antagonists, and antacids. However, these treatments have limitations, including short drug retention time in the stomach, low bioavailability, and potential side effects. Therefore, developing advanced drug delivery systems that offer improved therapeutic outcomes is crucial for effective ulcer management [02].

Polymeric nanoparticle-based drug delivery systems have emerged as a promising approach for enhancing the efficacy of peptic ulcer treatment. These systems provide controlled drug release, improved solubility, and increased mucosal adhesion, ensuring prolonged drug retention at the ulcer site [03]. Nanoparticles encapsulating antacid drugs such as magnesium hydroxide, aluminum hydroxide, or calcium carbonate can help neutralize gastric acid effectively while offering sustained release to maintain an optimal pH balance in the stomach over an extended period [04].

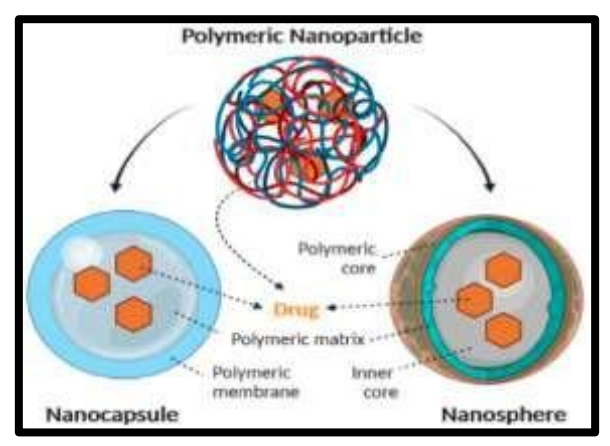


Fig no 01– The Diagrammatic representation of polymeric nanoparticles

The incorporation of biocompatible and biodegradable polymers, such as chitosan, poly(lactic-co-glycolic acid) (PLGA), and alginate, into nanoparticle formulations enhances the stability and mucoadhesive properties of the drug delivery system [05]. These polymers allow for the development of gastro-retentive formulations that can adhere to the gastric mucosa, thereby improving the local therapeutic effect and reducing the frequency of drug administration. This feature is particularly beneficial for patients who require long-term ulcer treatment [06].

Polymeric nanoparticle-based capsule composites can be designed to co-deliver antacid drugs along with gastroprotective agents or antibiotics to provide comprehensive ulcer treatment. For instance, the combination of an antacid with sucralfate or bismuth-based compounds can help form a protective barrier over the ulcer site, while the inclusion of antibiotics like amoxicillin or clarithromycin can aid in eradicating H. pylori infection. This multi-functional drug delivery approach enhances therapeutic efficacy and reduces the recurrence of ulcers [07].

Recent advancements in polymeric nanoparticle technology focus on optimizing formulation parameters, such as particle size, drug loading efficiency, and release kinetics, to ensure maximum therapeutic benefit. By leveraging these innovations, polymeric nanoparticle-based capsule composites offer a superior alternative to traditional antacid formulations, improving



patient compliance and treatment outcomes [08]. This novel approach holds great potential for revolutionizing peptic ulcer therapy by providing a more effective, targeted, and sustained drug delivery system [09].

MATERIAL & METHOD-

Lansoprazole, an active pharmaceutical ingredient (API), is manufactured by Cipla PVT. LTD at its Kurkumbh, Daund, Dist-Pune facility. The formulation of Lansoprazole involves various excipients sourced from different manufacturers. Polyvinyl Alcohol is provided by Yarrow Chem Product, Mumbai, while Methanol and Talcum Powder are supplied by Thomas Baker (Chemicals) PVT. LTD. Chitosan comes from Chemdyes Corporations, and Methyl Cellulose is produced by Research Laboratory, Mumbai. Macrocrystalline Cellulose is manufactured by Laboratories Regent & Fine Chemicals, Magnesium Stearate by Pallay Chemicals & Solvent PVT. LTD., and Mannitol by Moly-chem, Mumbai. These excipients play a crucial role in stabilizing, binding, and enhancing the formulation's effectiveness.

PREFORMULATION STUDY-

Solubility- The solubility of Lansoprazole is qualitatively determined by adding a solvent in small increments to a fixed amount of API (or vice versa), followed by vigorous shaking and visual observation [10]. Once dissolved, 1 mL of the mixture is diluted to 10 mL with 0.1N HCl as the dissolution medium. The absorbance of the prepared solution is recorded using UV spectroscopy at a specific wavelength [11]. The obtained absorbance values are plotted on a graph to analyze the solubility profile, helping to identify the most suitable organic solvent for nanoparticle preparation [12].

Melting Point-

The melting point of a substance is determined using the Thiele tube method, which involves filling the tube with liquid and heating it uniformly [13]. A capillary tube containing the sample is immersed in the liquid, and the temperature is gradually increased. As the sample melts, the temperature is recorded, giving the melting point. This method ensures accurate and consistent results for determining the thermal properties of a substance [14].

UV Analysis of Drug (API) Sample-

For Acidic Gastric Media -

A 1000 PPM stock solution is prepared using acidic gastric fluid (0.1N HCl), which is then diluted to obtain a 10 PPM solution. Further dilutions are made to prepare 2, 4, 6, 8, and 10 PPM solutions [15]. The absorbance of these solutions is measured under UV spectroscopy at a specific wavelength. The recorded absorbance values are then plotted on a graph to establish a standard calibration curve, aiding in the analysis of concentration-dependent absorbance behaviour [16].

For The Basic Gastric Media-

A 7.4 pH phosphate buffer is prepared by dissolving 8 g of sodium chloride in distilled water, followed by adding 1.44 g of disodium hydrogen phosphate, 0.24 g of potassium dihydrogen phosphate, and 0.2 g of potassium chloride. The solution volume is adjusted to 1000 mL with distilled water, and the pH is checked and adjusted if necessary [17]. Using this buffer, a 1000 PPM stock solution is prepared and further diluted to obtain a 10 PPM solution. Additional dilutions (2, 4, 6, 8, and 10 PPM) are made, and their absorbance is measured under UV spectroscopy at a specific wavelength [18]. The absorbance values are plotted on a graph to analyze the concentration-dependent behaviour [19].

FTIR Study (Drug Excipients Study)-

FTIR spectroscopy generates an absorbance spectrum that identifies unique chemical bonds and molecular structures in a sample. The absorbance peaks correspond to different functional groups, such as alkanes, ketones, and acid chlorides, based on their infrared absorption at specific wavelengths [20]. To conduct the study, the drug sample is weighed, placed in a sample holder, and analyzed under the FTIR spectrometer. The spectrum is



recorded across different IR regions, allowing the identification of functional groups by studying their stretching and vibration patterns [21]. This analysis is crucial for determining drug compatibility with polymers and other excipients [22].

METHOD-

Formulation Table-

Table no 01- Formulation Table

In andian4	Formulations						
Ingredient	F1	F2	F3	F4	F5	F6	
API- Lansoprazole (mg)	30	30	30	30	30	30	
Chitosan (%)	0.1	0.5	1.0	-	-	-	
Methyl Cellulose (%)	-	-	-	0.1	0.5	1.0	
Polyvinyl Alcohol (%)	0.25	0.25	0.25	0.25	0.25	0.25	
Organic Phase Aqueous Phase & Ratio (ml)	1:10	1:10	1:10	1:10	1:10	1:10	
Capsule Base (mg)	Q. S. 250mg						

Method of Preparation-

The solvent evaporation method is used to prepare nano polymeric nanoparticles by combining organic and aqueous phases in a 1:10 ratio [23]. The organic phase consists of a polar organic solvent (ethanol) mixed with a polymer (chitosan or methyl-cellulose) and the API (Lansoprazole), while the aqueous phase contains a surfactant and an aqueous solvent mixture [24]. Both phases are prepared separately and then mixed, followed by particle size reduction using a probe sonicator for 35 minutes at 40°C. The solvent is removed using a magnetic stirrer, allowing nano-droplet formation over 3 hours at room temperature [25]. Further solvent removal is done using a rotary evaporator for 5 minutes [26]. The nanoparticles are then collected via ultracentrifugation at 12,000 RPM, washed three times with deionized water, and stabilized with a 5% sugar solution as a cryoprotectant [27]. The final nanoparticles are stored using freeze-drying overnight [28]. The prepared nanoparticles are then mixed with a capsule base to form polymeric-coated nanoparticle capsules [29].

CHARACTERIZATION OF NANOPARTICLES-

The pH of Suspension-

To measure the pH of a sample, first place the electrode in an appropriate buffer solution and begin reading. Press the measure button to start calibration and set the pH meter to the buffer's known pH value once the reading stabilizes [30]. Repeat this calibration process for accuracy. After calibration, immerse the electrode in the sample solution and press the measure button again to determine the sample's pH. Ensure the reading stabilizes before recording the final pH value [31].

Particle size analysis-

Particle size analysis determines the size distribution of particles in a sample and is applicable to solids, suspensions, emulsions, and aerosols [32]. Various methods are used for measurement, with the Laser Diffraction Method being a common technique. In the case of formulated nano-suspensions, particle size is measured using the Malvern instrument, which utilizes laser diffraction to analyze particle distribution accurately [33]. This method helps in optimizing formulation properties, ensuring stability, and achieving desired drug delivery characteristics [34].



Steps for particle size measurement by an instrument-

Liquid suspensions containing nanoparticles can be analyzed using a recirculating cell, where dispersing agents like 0.1% Calgon or sodium hexametaphosphate solution (for TiO₂) are added to ensure proper dispersion [35]. This method is ideal for measuring particle size in aqueous or organic suspensions. A small sample (1-2 g or mL) is placed in the sample holder, ensuring a representative portion is analyzed [36]. The entire sample passes through a laser beam, and diffraction data from all particles is collected. This technique is non-destructive and non-intrusive, allowing for sample recovery if needed, making it highly effective for valuable materials [37].

Zeta potential-

A 1 mL sample of a nanoparticle-containing suspension was dispersed in double-distilled water to ensure proper dilution [38]. To prevent agglomeration of nanoparticles, the dispersed solution was sonicated in an ultrasonic bath for 5 minutes. After sonication, the sample was transferred into a glass cuvette and placed in the sample holder of a Zetasizer instrument [39]. The zeta potential, which provides insights into the stability and surface charge of the nanoparticles, was then measured to assess the dispersion quality and ensure stability of the suspension [40].

Drug Entrapment Efficiency (DEE)-

To determine the drug entrapment efficiency, 5 mL of the prepared nano-suspension containing nanoparticles was placed in a test tube and centrifuged at 4000 RPM for 20 minutes [41]. After centrifugation, the supernatant was collected and filtered to remove any suspended particles [42]. A 1 mL sample of the filtered supernatant was then diluted with water up to 10 mL. The absorbance of the diluted supernatant was measured at a wavelength of 298 nm to quantify the amount of unentrapped drug [43]. This data is used to calculate the entrapment efficiency of the nanoparticles in the formulation [44].

EVALUATION

(polymeric nanoparticles capsule composite)-

Pre-Capsule Filling Parameters Study-

The angle of Repose (Ø)

The angle of repose is used to measure the frictional force in loose powders or granules by determining the maximum angle between the surface of a pile of the material and the horizontal plane [45]. It is calculated using the formula $\text{Tan } \emptyset = \text{H/r}$, where \emptyset is the angle of repose, H is the height of the cone formed by the powder, and r is the radius of the cone's base. A higher angle indicates more resistance to flow, while a lower angle suggests better flowability. This test is important for assessing the handling and processing properties of powders in various formulations.

In this method, a funnel is filled to the brim with the test sample, and the granules are allowed to flow smoothly through the orifice under the influence of gravity [46]. The powder forms a cone on a graph sheet, and the area of the cone is measured to evaluate the flowability of the granules. Additionally, the height of the pile is measured to further assess the material's flow properties [47]. This test helps determine the ease with which granules can flow, which is important for processing and handling during formulation [48].

Bulk Density & Tap Density -

Bulk density (LBD) and tapped bulk density (TBD) of the drug or dosage form blends were determined using a bulk density apparatus [49]. The pure drug was first passed through a #18 sieve to break any clumps. A precisely weighed 5 g sample of the drug or 25 g of the polymers was placed in a 100 mL graduated measuring cylinder, and the initial volume was recorded. The cylinder was then tapped 200 times from a distance of 14 ± 2 mm, and the tapped volume was measured [50]. This process was repeated for an additional 200 taps, and the final tapped volume was recorded. The same procedure was performed for the powder



blends of the dosage form. The bulk density (LBD) and tapped bulk density (TBD) were calculated in g per mL, providing important information on the flowability and compressibility of the materials [51].

Bulk Density = weight of the powder/volume of the packing Tab Density = weight of the powder/tapped volume of the packing

Hausner ratio-

The Hausner ratio is a measure of the flowability of a powder, calculated using the formula: Hausner ratio = Tapped Bulk Density (TBD) / Loose Bulk Density (LBD). A Hausner ratio less than 1.25 indicates that the powder has better flow properties, meaning it flows more easily and is less prone to clumping or compaction [52]. Conversely, a ratio greater than 1.25 suggests poorer flowability, indicating that the powder may be more prone to problems like segregation or poor uniformity in formulation [53]. This ratio is important for assessing how powders will behave during processing, handling, and encapsulation [54].

Post-Capsule Filling Parameters Study-Weight Variation & Content Uniformity-

The weight variation test is a statistical quality control method used to ensure uniformity in dosage units, supporting product safety, identity, and quality [55]. In food and beverage production, this test helps confirm that fill quantities meet legal requirements. For capsules, each unit is weighed individually. The capsule is carefully opened without damaging the shell, and the contents are removed completely. The weight of the shell is then measured, and the weight of the contents is calculated by subtracting the shell's weight [56]. This procedure is repeated for 20 randomly selected capsules. The average weight is determined, and the weight variation is calculated using the appropriate formula to assess the consistency of the dosage units [57].

Disintegration study -

To prepare 1000 mL of both acidic and basic gastric fluids, 0.1N HCl solution is prepared for the acidic fluid, and a 7.4 pH buffer solution is prepared for the basic fluid. Both solutions are placed in separate disintegration flasks, and the temperature is maintained at body temperature (37°C) [58]. The capsule is placed in a test tube within the disintegration apparatus, and the instrument is started. The disintegration time is observed by monitoring the time taken for the capsule to break down completely in each solution [59]. This test helps evaluate the dissolution characteristics and the performance of the capsule under different gastric conditions [60].

Drug content-

Five capsules were weighed and emptied to obtain a powder equivalent to 150 mg of Lansoprazole [61]. The powder was dissolved in a suitable amount of buffer solution, and the resulting solution was filtered to remove any impurities [62]. The filtered solution was then appropriately diluted to bring the concentration within measurable limits [63]. The drug content of the sample was determined by measuring the absorbance using a UV spectrophotometer at a specific wavelength, which allowed for accurate quantification of the Lansoprazole content in the sample [64].

In vitro study-

Dissolution is the process by which a capsule or other dosage form dissolves into a solution, and it plays a crucial role in determining the rate at which the drug is released from the dosage form. This systematic procedure is essential for evaluating bioavailability, as it helps assess how quickly and efficiently the drug is absorbed into the body [65]. Dissolution testing is also important for ensuring the quality of the product, as it directly correlates with the drug's performance. It is a vital quality control technique used to monitor the consistency and effectiveness of pharmaceutical products throughout their shelf life [66].

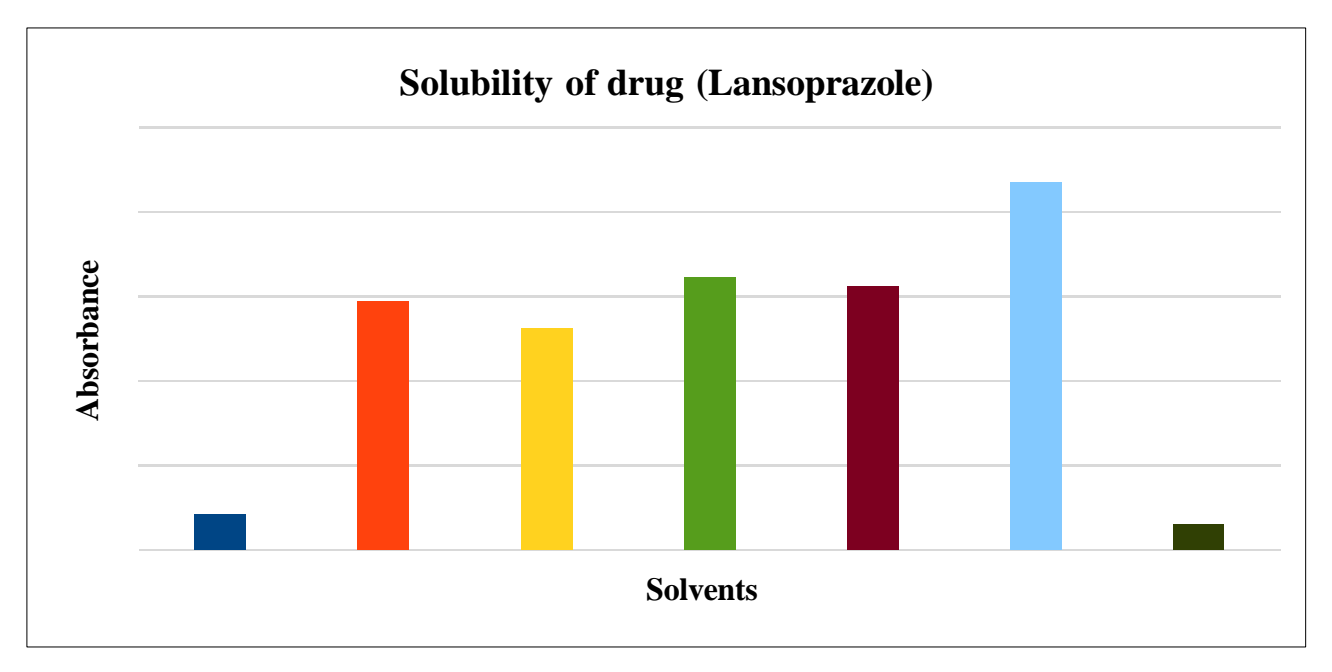


RESULTS & DISCUSSIONS-

Pre formulations-

Table no 02- The Table contains the Solubility of API with absorbance

Solvent	Absorbance
Ethyl acetate	0.0021
Chloroform	0.0147
Methanol	0.0131
Dimethyl Sulphoxide	0.0161
Methyl Chloride	0.0156
Ethanol	0.0217
Water	0.0015



Graph no 1 - Solubility Graph of drug API -Lansoprazole

The table presents the absorbance values for different solvents used to dissolve an API, which reflects the solubility of the drug in each solvent. Ethyl acetate has the lowest absorbance (0.0021), indicating lower solubility, while ethanol shows the highest absorbance (0.0217), suggesting better solubility of the API in ethanol. Other solvents like chloroform (0.0147), methanol (0.0131), dimethyl sulfoxide (0.0161), and methyl chloride (0.0156) exhibit moderate absorbance values, indicating varying degrees of solubility. Water, with an absorbance of 0.0015, shows the least solubility for the API. These absorbance values are useful for selecting the optimal solvent for further formulation and analysis.

Melting Point-

Table no 03- The table contains the observation of the melting point.

API Sample	Reference MP °C	Observed MP°C	Final MP °C
Lansoprazole		166	
	166	168	166-167
		166	



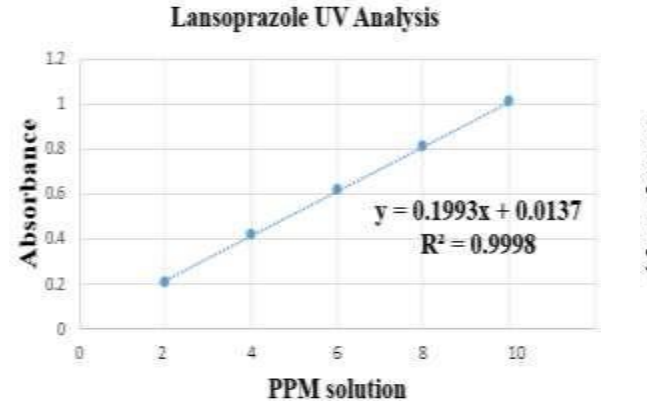
The table shows the melting point observations for the API sample, Lansoprazole. The reference melting point (MP) of Lansoprazole is 166°C, and the observed melting points for the sample were consistent, with values of 166°C and 168°C. The final observed melting point range is 166-167°C, indicating that the sample's melting point closely matches the reference value. This consistency in melting point suggests that the Lansoprazole sample is pure and that it exhibits the expected thermal properties, which is important for its identification and quality control.

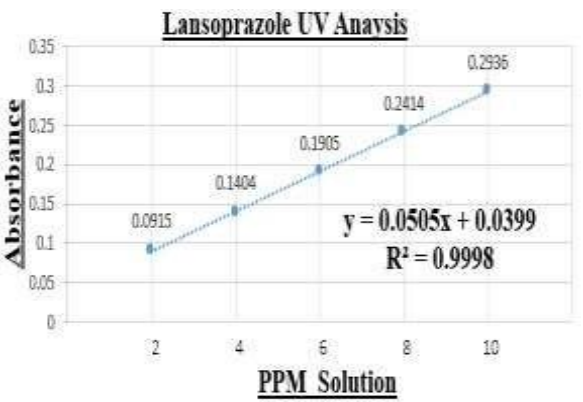
UV Analysis of Drug (API) Sample-

For Acidic Gastric Media-

Table no 04- The Table contains the absorbance of particular samples for acidic media (lambda max 298).

PPM Solution	Absorbance
2 ppm	0.0915
4 ppm	0.1404
6 ppm	0.1905
8 ppm	0.2414
10 ppm	0.2936





Graph no 2 - The Graph Contains Graph no 3 - The Graph Contains Lansoprazole UV Analysis for Acidic lansoprazole UV Analysis for Basic Media. Media

For Basic Gastric Media-

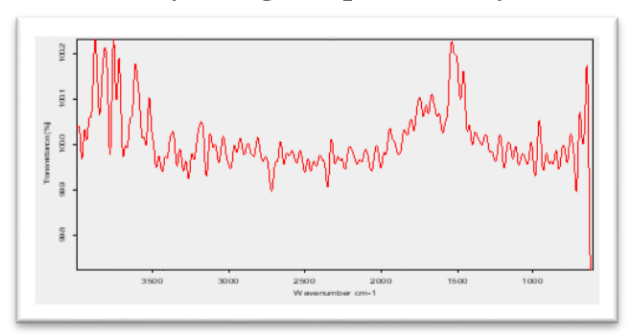
Table no 05- The Table contains the absorbance of particular samples for basic media.

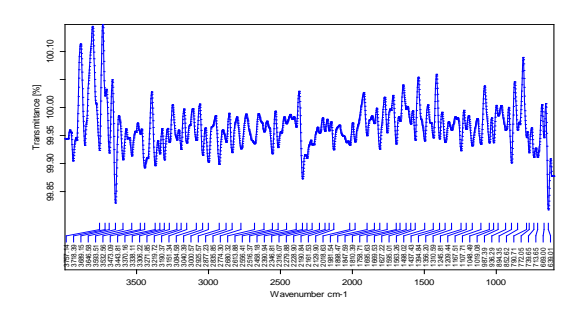
PPM Solution	Lansoprazole
2 ppm	0.2081
4 ppm	0.4154
6 ppm	0.6181
8 ppm	0.8082
10 ppm	1.0083



The tables show the absorbance values of Lansoprazole at different concentrations in both acidic and basic media, with absorbance measured at a lambda max of 298 nm. In acidic media, the absorbance increases with concentration, starting at 0.0915 for the 2 ppm solution and reaching 0.2936 for the 10 ppm solution, indicating a linear relationship between concentration and absorbance. In basic media, the absorbance values are higher compared to the acidic media for the same concentrations, with the 2 ppm solution having an absorbance of 0.2081 and the 10 ppm solution showing an absorbance of 1.0083. This suggests that Lansoprazole has different absorbance characteristics in acidic versus basic conditions, which could be important for understanding its behavior in various dissolution environments.

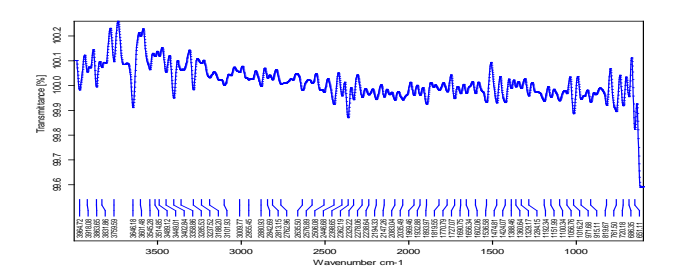
FTIR Study (Drug Excipients Study)-

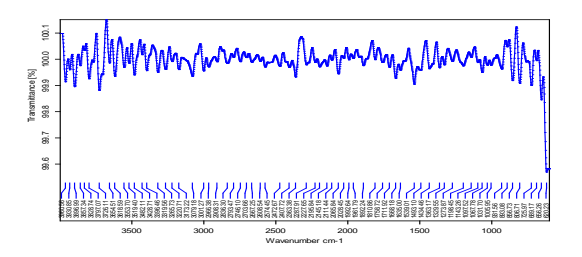




Graph no 4 - The Graph Contains lansoprazole drug (API) Sample FTIR study

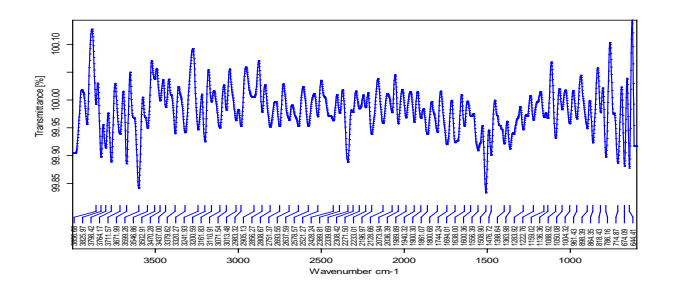
Graph no 5 - The Graph Contains lansoprazole with Xanthan Gum Sample FTIR study

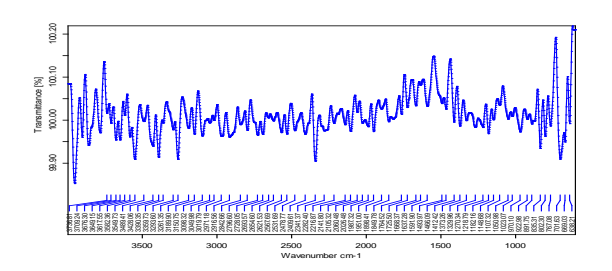




Graph no 6 - The Graph Contains Lansoprazole with chitosan Sample FTIR study

Graph no 7 - The Graph Contains lansoprazole with Capsule Base Sample FTIR study





Graph no 8 - The Graph Contains lansoprazole with Methyl Cellulose Base Sample FTIR study

Graph no 9 - The Graph Contains lansoprazole with Ethyl Cellulose Base Sample FTIR study



Table no 06- The interpretation records of drug (API) samples & the Excipients

Complex	Stretching (cm ⁻¹)					
Samples	S=O	C-N	С-Н	N-H		
Lansoprazole	1016.21	1284.15	2762.96	3188.20		
Lansoprazole + Xanthan gum	1016.21	1284.15	2880.93	3285.53		
Lansoprazole + chitosan	1167.51	1245.81	2836.86	3306.22		
Lansoprazole + Capsule base	1088.92	1222.76	2808.67	3320.27		
Lansoprazole + Methyl cellulose	1182.16	1373.26	2796.60	3390.35		
Lansoprazole + ethyl cellulose	1067.78	1273.87	2746.10	3396.46		

The interpretation records of drug (Lansoprazole) samples and their corresponding excipients show the stretching frequencies (in cm-1) of various functional groups, including S=O, C-N, C-H, and N-H bonds. For pure Lansoprazole, the stretching frequencies are 1016.21 cm-1 (S=O), 1284.15 cm-1 (C-N), 2762.96 cm-1 (C-H), and 3188.20 cm-1 (N-H). When Lansoprazole is combined with different excipients, such as Xanthan gum, chitosan, capsule base, methyl cellulose, and ethyl cellulose, shifts in these frequencies are observed, indicating possible interactions between the drug and excipients. For example, Lansoprazole with Xanthan gum shows an increase in the C-H stretch (2880.93 cm-1), while the combination with chitosan and methyl cellulose leads to shifts in both C-N and N-H stretches. These changes in the stretching frequencies help in understanding the compatibility and possible interactions between Lansoprazole and the excipients, which is important for formulation development.

Characterization of nanoparticles-

Physical appearance and pH determination of Suspension-

Table no 06- The physical appearance of the nanoparticles suspension

Formulations	Appearance	pН
F-1	Milky White	7.4
F-2	Milky White	7.0
F-3	Milky White	6.8
F-4	Milky White	7.8
F-5	Milky White	7.2
F-6	Milky White	7.0

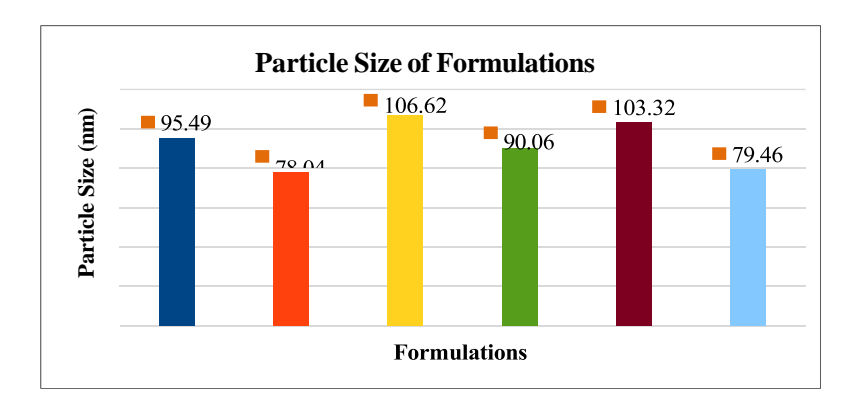
The physical appearance and pH of the nanoparticle suspensions for various formulations are recorded. All formulations (F-1 to F-6) appear milky white, indicating the presence of nanoparticles in suspension. The pH values of the formulations vary slightly, with F-1 having a pH of 7.4, F-2 a pH of 7.0, F-3 a pH of 6.8, F-4 a pH of 7.8, F-5 a pH of 7.2, and F-6 also a pH of 7.0. These pH values suggest that the formulations are within a neutral to slightly basic range, which is important for the stability and performance of the nanoparticles in suspension, ensuring their suitability for further applications.



Particle Size-

Table no 07- The table contains the different formulations particle size analysis

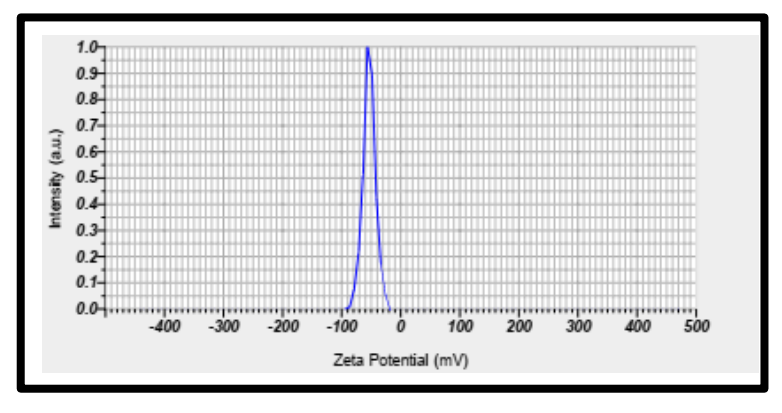
Formulation s	Particles Size (nm)	Particles Size (nm)	Particles Size (nm)	Mean (nm)
F1	84.12	94.28	108.08	95.49
F2	78.04	78.06	78.04	78.04
F3	102.22	112.06	105.56	106.62
F4	88.25	89.50	92.42	90.06
F5	109.82	102.02	98.13	103.32
F6	72.03	88.06	78.04	79.46



Graph no 10-The Graph contains the different formulations particle size analysis & its graphical presentation

The table presents the mean particle sizes (in nanometers) for different nanoparticle formulations, measured through particle size analysis. Formulation F1 has a mean particle size of 95.49 nm, F2 has 78.04 nm, F3 has 106.62 nm, F4 has 90.06 nm, F5 has 103.32 nm, and F6 has 79.46 nm. These values indicate slight variations in the particle sizes across the different formulations. Smaller particle sizes, like those of F2 and F6, may enhance the surface area for drug delivery, improving bioavailability, while larger particles, like those in F3 and F5, may impact the release rate and stability. This particle size distribution is crucial for determining the efficacy, stability, and performance of the nanoparticle formulations in their intended applications.

Zeta Potential



Graph no 11 - The graph mention that the ideal zeta potential of formulation

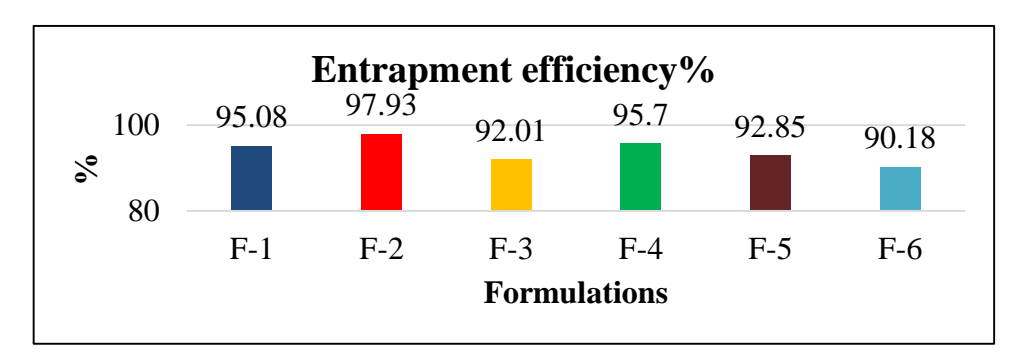


The zeta potential of the nanoparticle suspension was measured using a zeta sizer and found to be 54.3 mV, which is considered acceptable for stability. According to standard guidelines, a zeta potential greater than +30 mV or less than -30 mV indicates a stable colloidal suspension. A zeta potential value of -54.3 mV suggests strong electrostatic repulsion between the nanoparticles, which helps prevent aggregation and ensures that the suspension remains stable over time. This value is crucial for maintaining the uniformity and effectiveness of the nanoparticle formulation in its intended application.

Encapsulation Efficiency-

Table no 08 - The Encapsulations efficiency of various formulations

Formulations	Entrapment efficiency%
F-1	95.08
F-2	97.93
F-3	92.01
F-4	95.70
F-5	92.85
F-6	90.18



Graph no 12 - The Entrapment efficiency of various formulations in graphical form

The encapsulation efficiency of various nanoparticle formulations is recorded in the table, showing the percentage of drug successfully encapsulated within the nanoparticles. Formulation F-2 exhibits the highest entrapment efficiency at 97.93%, indicating that it successfully retains a larger portion of the drug within the nanoparticles. Other formulations, such as F-1 (95.08%), F-4 (95.70%), and F-5 (92.85%), also demonstrate high encapsulation efficiencies, suggesting efficient drug incorporation. Formulations F-3 (92.01%) and F-6 (90.18%) have slightly lower efficiencies, but still show favorable encapsulation. High encapsulation efficiency is important for ensuring that the therapeutic drug dose is delivered effectively and consistently in nanoparticle-based drug delivery systems.

Evaluation (polymeric nanoparticles capsule composite)-

Pre-Capsule Filling Parameters Study-

Table no 09– The all pre capsule filling parameter study in the table

Formulatio ns	Angle of repose Degree (°)	Bulk Density (mg/ml)	Tap Density (mg/ml)	Hausner's Ratio
F1	29.74	0.511	0.625	1.250
F2	27.75	0.4761	0.5264	0.9045
F3	27.83	0.4673	0.5883	0.7944
F4	33.66	0.4902	0.5435	0.9019

F5	31.21	0.4814	0.6994	0.6883
F6	32.82	s0.4579	0.4909	0.9327

The pre-capsule filling parameters for various formulations are summarized in the table, providing insights into the powder flow characteristics and compactibility of the formulations. The angle of repose, which indicates powder flowability, ranges from 27.75° (F2) to 33.66° (F4), with formulations F1, F3, and F5 having moderate angles of repose, suggesting acceptable flow properties. The bulk density values, which represent the mass of the powder per unit volume, range from 0.4579 mg/ml (F6) to 0.511 mg/ml (F1). Tap density values, which are measured after tapping to compact the powder, show a range from 0.4909 mg/ml (F6) to 0.6994 mg/ml (F5). The Hausner's ratio, which is a measure of flowability and cohesiveness of the powder, indicates that formulations with a ratio less than 1.25 (F2, F3) have better flow properties, while ratios greater than 1.25 (F1, F4, F5) may suggest more compacted powders with potentially poorer flow. Overall, these parameters help assess the suitability of the formulations for capsule filling, as they directly impact the ease of processing and uniformity of capsule content.

Post-Capsule Filling Parameters Study-Weight Variation-

Table no 10- The weight variation of various formulation

Cracification	Weight of Capsules (mg)					
Specification	F1	F2	F3	F4	F5	F6
Total weight	4989	4998	4993	4990	4992	4993
Averages weight	249.45	249.9	249.65	249.5	249.6	249.65
Upper limit	252	251	252	252	253	251
Lower Limit	247	247	247	247	246	247
% Variation	2.004	1.6	2.002	2.004	2.804	1.602

The weight variation of various capsule formulations is presented in the table, with the total and average capsule weights, along with the upper and lower limits and the percentage variation for each formulation. All formulations show average capsule weights around 249 mg, with slight variations ranging from 249.45 mg (F1) to 249.65 mg (F3 and F6). The upper and lower weight limits are set close to 250 mg, with slight differences across formulations, such as 252 mg (upper limit for F1 and F3) and 246-253 mg (lower and upper limits for F5). The percentage variation of capsule weight indicates the uniformity of the formulation, with F2 and F6 showing the lowest variation (1.6% and 1.602%, respectively), while F5 exhibits the highest variation (2.804%). These results suggest that most formulations are within acceptable limits for weight variation, ensuring consistent dosing and quality for the capsules.

Disintegration Test-

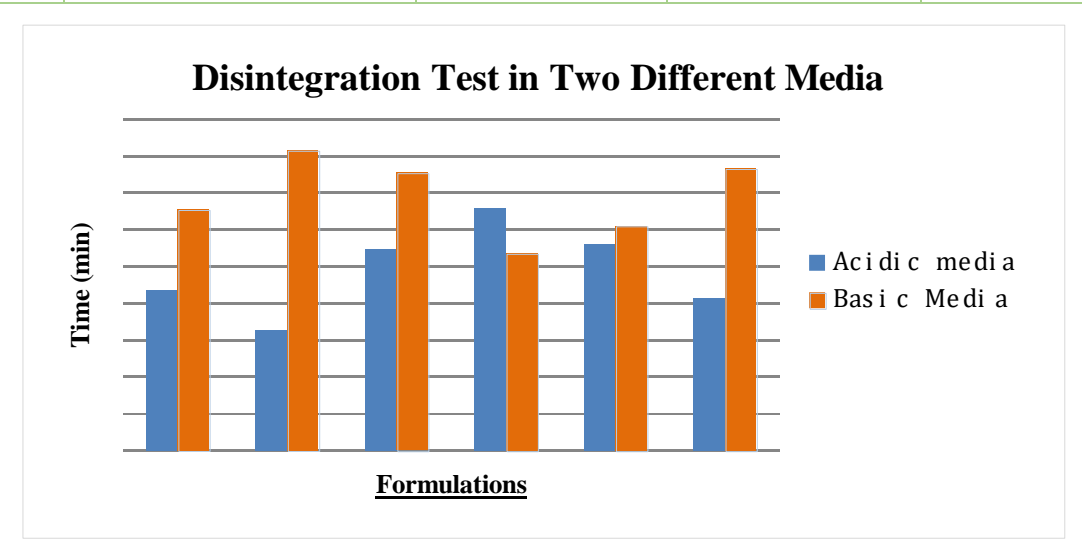
Table no11- The Disintegration time of various formulations in basic media

Formulations	Time of Disintegration of Capsules (min) for Acidic Gastric Media-Stomach				
	C1	C2	C3	Mean	
F1	10.45	7.25	8.38	8.693	
F2	6.10	6.58	7.01	6.563	
F3	11.15	15.59	6.10	10.95	
F4	16.0	6.10	17.25	13.16	
F5	14.26	13.33	6.10	11.23	
F6	8.58	6.10	10.12	8.27	



Table no12– The Disintegration time of various formulations in basic media

Capsule	Time of Disintegration of Capsules (min) for Basic Gastric Media- Intestine				
	C1	C2	C3	Mean	
F 1	13.42	12.44	13.48	13.12	
F2	16.23	16.02	16.15	16.34	
F3	16.52	13.35	15.42	15.12	
F4	17.02	6.10	9.07	10.73	
F5	14.08	12.27	10.34	12.23	
F6	19.28	12.20	14.51	15.34	



Graph no 13- The graphical representation of disintegration time of formulation in two different media

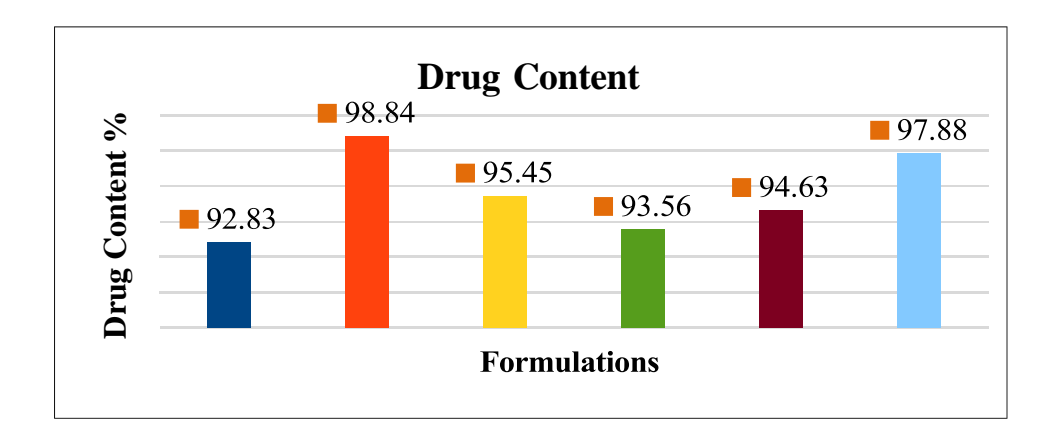
The Determination of disintegration time take place as per standard method & instrument take place in that due to the extended-release capsule the method followed by two different medium have to done i.e., Acidic media & basic media from the Stomach & intestine respectively as per observation the capsule disintegrates in acidic media in short duration & basic media in long duration

Drug Content-

Table no 13- The Drug content in the formulation in percentage

Formulations	Drug Content (%)		
F1	92.83		
F2	98.84		
F3	95.45		
F4	93.56		
F5	94.63		
F6	97.88		





Graph no 14- The Percentage Drug content in the formulationThe drug content in various formulations is presented in the table, showing the percentage of active pharmaceutical ingredient (API) present in each capsule formulation. Formulation F2 has the highest drug content at 98.84%, indicating that it contains the most accurate amount of the active ingredient. Other formulations, such as F3 (95.45%), F5 (94.63%), and F6 (97.88%), also show relatively high drug content, suggesting good consistency in drug encapsulation. Formulations F1 (92.83%) and F4 (93.56%) have slightly lower drug content, but still fall within an acceptable range for pharmaceutical formulations. Overall, these results indicate that all formulations are within an appropriate range for drug content, ensuring the intended therapeutic effect for each capsule.

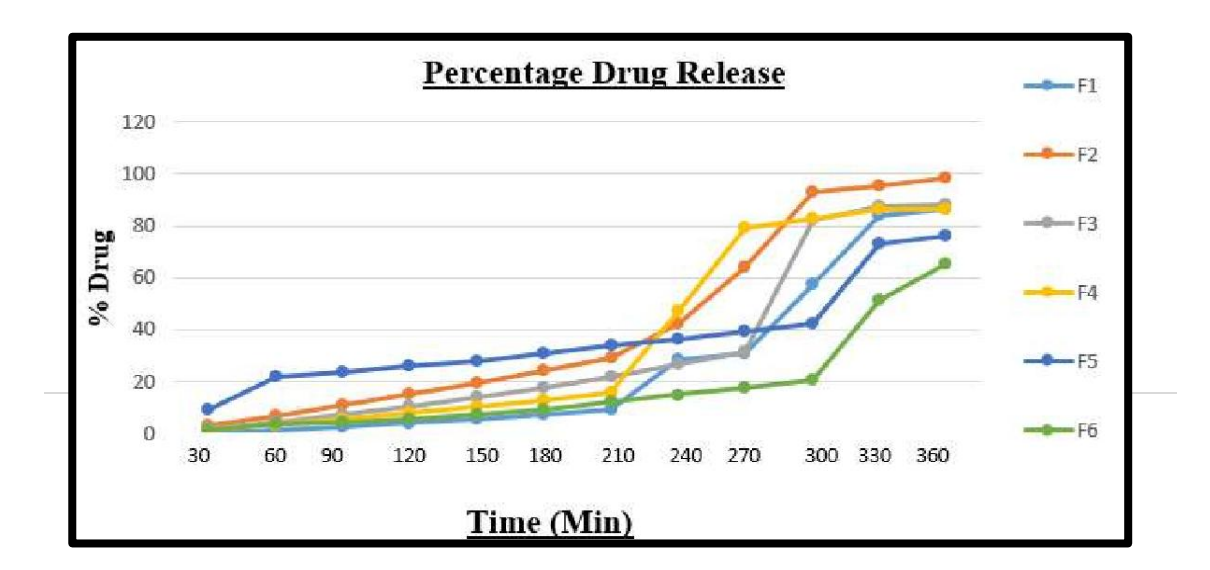
The drug content in various formulations is presented in the table, showing the percentage of active pharmaceutical ingredient (API) present in each capsule formulation. Formulation F2 has the highest drug content at 98.84%, indicating that it contains the most accurate amount of the active ingredient. Other formulations, such as F3 (95.45%), F5 (94.63%), and F6 (97.88%), also show relatively high drug content, suggesting good consistency in drug encapsulation. Formulations F1 (92.83%) and F4 (93.56%) have slightly lower drug content, but still fall within an acceptable range for pharmaceutical formulations. Overall, these results indicate that all formulations are within an appropriate range for drug content, ensuring the intended therapeutic effect for each capsule.

In Vitro study-

Table no 14- Contain Percentage drug release time at various time intervals Time (Min)

Time (Min)	F1	F2	F3	F4	F5	F6
30	0.07129	3.47523	2.24554	1.65149	9.56436	1.18812
60	1.27723	7.06929	4.71683	3.52871	22.099	3.56436
90	2.6495	10.901	7.18812	5.40594	23.9762	4.42574
120	4.14059	15.0653	10.4851	8.10891	25.8772	5.91089
150	5.67327	19.4138	13.901	10.2594	28.0277	7.54455
180	7.26535	24.0356	17.9287	13.099	30.8673	9.33267
210	9.11287	29.1921	22.1584	15.9624	33.6653	12.1307
240	28.598	42.1426	26.804	46.9129	36.5228	14.9881
270	31.1644	63.8851	31.5683	79.3485	39.4634	17.9287
300	57.4218	92.697	82.1822	82.8238	42.4396	20.905
330	84.2139	95.3703	87.4218	86.299	72.8554	51.3208
360	86.2636	98.452	88.4254	86.584	75.954	65.2267





Graph no 15- Contain Percentage drug release time at various time intervals in graphical form

The table shows the percentage of drug release over time for various formulations at different time intervals. At 30 minutes, the drug release is minimal across all formulations, with F1, F2, F3, and F4 showing very low drug release (ranging from 0.071% to 3.475%), while F5 releases 9.564% and F6 releases 1.188%. However, at 360 minutes (6 hours), there is a significant increase in drug release, with formulation F2 exhibiting the highest release at 98.45%, followed by F3 (88.43%) and F4 (86.58%). F1, F5, and F6 show lower releases, ranging from 75.95% (F5) to 86.26% (F1). These results suggest that F2 demonstrates the fastest and most complete drug release, while other formulations exhibit more controlled or slower release profiles, which could be tailored to different therapeutic needs.

CONCLUSION-

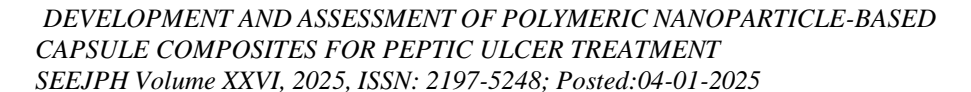
The formulation and evaluation of polymeric nanoparticle capsule composites, using both natural polymer chitosan and synthetic polymer methylcellulose, revealed that formulation F2 was the most optimized compared to others. This formulation demonstrated superior characteristics such as the smallest particle size (78.04 nm), the highest entrapment efficiency (97.93%), a strong zeta potential (53.4 mV), and excellent drug content (98.84%). Additionally, its in vitro drug release profile showed the highest release rate (98.45%) over 6 hours, outperforming all other formulations. When compared to the marketed traditional lansoprazole capsules, F2 showed significantly better drug release performance. Animal studies further confirmed that the optimized formulation effectively treated inflammation and ulcerative conditions in the stomach, exhibiting superior therapeutic efficacy compared to other formulations. These results suggest that F2 is a highly promising candidate for enhanced drug delivery and therapeutic outcomes.

CONFLICTS OF INTEREST-

There are no conflicts of interest and disclosures regarding the manuscript.

REFERENCES-

1. Safarov T, Kiran B, Bagirova M, Allahverdiyev AM, Abamor ES. An overview of nanotechnology-based treatment approaches against Helicobacter Pylori. Expert Review of Anti-infective Therapy. 2019 Oct 3;17(10):829–40.





- 2. Vodnik VV, Šaponjić Z, Džunuzović JV, Bogdanović U, Mitrić M, Nedeljković J. Anisotropic silver nanoparticles as filler for the formation of hybrid nanocomposites. Materials Research Bulletin. 2013 Jan;48(1):52–7.
- 3. Abdel-Mohsen AM, Abdel-Rahman RM, Hrdina R, Imramovský A, Burgert L, Aly AS. Antibacterial cotton fabrics treated with core—shell nanoparticles. International Journal of Biological Macromolecules. 2012 Jun;50(5):1245–53.
- 4. El-Rafie MH, Mohamed AA, Shaheen ThI, Hebeish A. Antimicrobial effect of silver nanoparticles produced by fungal process on cotton fabrics. Carbohydrate Polymers. 2010 May 5;80(3):779–82.
- Carvalho SM, Oliveira AAR, Lemos EMF, Pereira MM. Bioactive Glass Nanoparticles for Periodontal Regeneration and Applications in Dentistry. In: Nanobiomaterials in Clinical Dentistry [Internet]. Elsevier; 2013 [cited 2025 Feb 6]. p. 299–322. Available from: https://linkinghub.elsevier.com/retrieve/pii/B9781455731275000155
- 6. Singh P, Kim YJ, Zhang D, Yang DC. Biological Synthesis of Nanoparticles from Plants and Microorganisms. Trends in Biotechnology. 2016 Jul;34(7):588–99.
- 7. Lv Q, Zhang B, Xing X, Zhao Y, Cai R, Wang W, et al. Biosynthesis of copper nanoparticles using Shewanella loihica PV-4 with antibacterial activity: Novel approach and mechanisms investigation. Journal of Hazardous Materials. 2018 Apr;347:141–9.
- 8. Kuppusamy P, Yusoff MM, Maniam GP, Govindan N. Biosynthesis of metallic nanoparticles using plant derivatives and their new avenues in pharmacological applications An updated report. Saudi Pharmaceutical Journal. 2016 Jul;24(4):473–84.
- 9. Joos A, Rümenapp C, Wagner FE, Gleich B. Characterisation of iron oxide nanoparticles by Mössbauer spectroscopy at ambient temperature. Journal of Magnetism and Magnetic Materials. 2016 Feb;399:123–9.
- 10. Shobana MK, Sankar S, Rajendran V. Characterization of Co0.5Mn0.5Fe2O4 nanoparticles. Materials Chemistry and Physics. 2009 Jan;113(1):10–3.
- 11. Boselli L, Lopez H, Zhang W, Cai Q, Giannone VA, Li J, et al. Classification and biological identity of complex nano shapes. Commun Mater. 2020 Jun 12;1(1):35.
- 12. Roman SG, Chebotareva NA, Kurganov BI. Concentration dependence of chaperone-like activities of α-crystallin, αB-crystallin and proline. International Journal of Biological Macromolecules. 2012 Jun;50(5):1341–5.
- 13. Sasaki T, Ohara S, Naka T, Vejpravova J, Sechovsky V, Umetsu M, et al. Continuous synthesis of fine MgFe2O4 nanoparticles by supercritical hydrothermal reaction. The Journal of Supercritical Fluids. 2010 Jun;53(1–3):92–4.
- 14. Yadi M, Mostafavi E, Saleh B, Davaran S, Aliyeva I, Khalilov R, et al. Current developments in green synthesis of metallic nanoparticles using plant extracts: a review. Artificial Cells, Nanomedicine, and Biotechnology. 2018 Nov 12;46(sup3):336–43.
- 15. Smitha KT, Nisha N, Maya S, Biswas R, Jayakumar R. Delivery of rifampicin-chitin nanoparticles into the intracellular compartment of polymorphonuclear leukocytes. International Journal of Biological Macromolecules. 2015 Mar;74:36–43.
- 16. Mayence A. Design and characterization of nanoparticles and their assemblies: Transmission electron microscopy investigations from atomic to mesoscopic length scales. Stockholm: Department of Materials and Environmental Chemistry (MMK), Stockholm University; 2016. 66 p.
- 17. Chen RH, Phuoc TX, Martello D. Effects of nanoparticles on nanofluid droplet evaporation. International Journal of Heat and Mass Transfer. 2010 Sep;53(19–20):3677–82
- 18. Berteloot G, Hoang A, Daerr A, Kavehpour HP, Lequeux F, Limat L. Evaporation of a sessile droplet: Inside the coffee stain. Journal of Colloid and Interface Science. 2012 Mar;370(1):155–61.
- 19. Chalikwar SS, Belgamwar VS, Talele VR, Surana SJ, Patil MU. Formulation and evaluation of Nimodipine-loaded solid lipid nanoparticles delivered via lymphatic

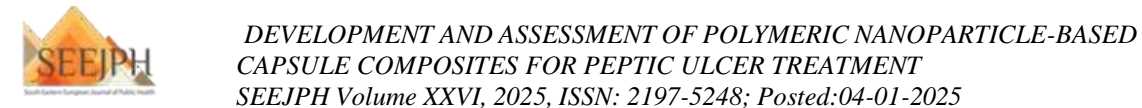




- transport system. Colloids and Surfaces B: Biointerfaces. 2012 Sep;97:109–16.
- 20. Hassouneh W, MacEwan SR, Chilkoti A. Fusions of Elastin-Like Polypeptides to Pharmaceutical Proteins. In: Methods in Enzymology [Internet]. Elsevier; 2012 [cited 2025 Feb 6]. p. 215–37. Available from: https://linkinghub.elsevier.com/retrieve/pii/B9780124160392000240
- 21. Yamaguchi R, Inoue Y, Tokunaga H, Ishibashi M, Arakawa T, Sumitani J ichi, et al. Halophilic characterization of starch-binding domain from Kocuria varians α-amylase. International Journal of Biological Macromolecules. 2012 Jan;50(1):95–102.
- 22. Zeng W, Miao B, Li T, Zhang H, Hussain S, Li Y, et al. Hydrothermal synthesis, characterization of h-WO3 nanowires and gas sensing of thin film sensor based on this powder. Thin Solid Films. 2015 Jun;584:294–9.
- 23. Brutin D. Influence of relative humidity and nano-particle concentration on pattern formation and evaporation rate of pinned drying drops of nanofluids. Colloids and Surfaces A: Physicochemical and Engineering Aspects. 2013 Jul;429:112–20.
- 24. Chaubey P, Mishra B. Mannose-conjugated chitosan nanoparticles loaded with rifampicin for the treatment of visceral leishmaniasis. Carbohydrate Polymers. 2014 Jan;101:1101–8.
- 25. Costa A, Sarmento B, Seabra V. Mannose-functionalized solid lipid nanoparticles are effective in targeting alveolar macrophages. European Journal of Pharmaceutical Sciences. 2018 Mar;114:103–13.
- 26. Jain A, Agarwal A, Majumder S, Lariya N, Khaya A, Agrawal H, et al. Mannosylated solid lipid nanoparticles as vectors for site-specific delivery of an anti-cancer drug. Journal of Controlled Release. 2010 Dec;148(3):359–67.
- 27. Wang Y, Li P, Truong-Dinh Tran T, Zhang J, Kong L. Manufacturing Techniques and Surface Engineering of Polymer Based Nanoparticles for Targeted Drug Delivery to Cancer. Nanomaterials. 2016 Feb 1;6(2):26.
- 28. Zhao Y, Yang X, Tian J, Wang F, Zhan L. Methanol electro-oxidation on Ni@Pd coreshell nanoparticles supported on multi-walled carbon nanotubes in alkaline media. International Journal of Hydrogen Energy. 2010 Apr;35(8):3249–57.
- 29. Sun B, Yeo Y. Nanocrystals for the parenteral delivery of poorly water-soluble drugs. Current Opinion in Solid State and Materials Science. 2012 Dec;16(6):295–301.
- 30. Piñón-Segundo E, Mendoza-Muñoz N, Quintanar-Guerrero D. Nanoparticles as Dental Drug-Delivery Systems. In: Nanobiomaterials in Clinical Dentistry [Internet]. Elsevier; 2013 [cited 2025 Feb 6]. p. 475–95. Available from: https://linkinghub.elsevier.com/retrieve/pii/B9781455731275000234
- 31. Bundschuh M, Filser J, Lüderwald S, McKee MS, Metreveli G, Schaumann GE, et al. Nanoparticles in the environment: where do we come from, where do we go to? Environ Sci Eur. 2018 Dec;30(1):6.
- 32. Strambeanu N, Demetrovici L, Dragos D, Lungu M. Nanoparticles: Definition, Classification and General Physical Properties. In: Lungu M, Neculae A, Bunoiu M, Biris C, editors. Nanoparticles' Promises and Risks [Internet]. Cham: Springer International Publishing; 2015 [cited 2025 Feb 6]. p. 3–8. Available from: https://link.springer.com/10.1007/978-3-319-11728-7
- 33. Strambeanu N, Demetrovici L, Dragos D, Lungu M. Nanoparticles: Definition, Classification and General Physical Properties. In: Lungu M, Neculae A, Bunoiu M, Biris C, editors. Nanoparticles' Promises and Risks [Internet]. Cham: Springer International Publishing; 2015 [cited 2025 Feb 6]. p. 3–8. Available from: https://link.springer.com/10.1007/978-3-319-11728-7_1
- 34. Khan I, Saeed K, Khan I. Nanoparticles: Properties, applications and toxicities. Arabian Journal of Chemistry. 2019 Nov;12(7):908–31.
- 35. Nassif M, El Askary F. Nanotechnology and Nanoparticles in Contemporary Dental Adhesives. In: Nanobiomaterials in Clinical Dentistry [Internet]. Elsevier; 2013 [cited



- 2025 Feb 6]. p. 131–64. Available from: https://linkinghub.elsevier.com/retrieve/pii/B9781455731275000076
- 36. Abu Abed OS, Chaw CS, Williams L, Elkordy AA. PEGylated polymeric nanocapsules for oral delivery of trypsin targeted to the small intestines. International Journal of Pharmaceutics. 2021 Jan;592:120094.
- 37. Xie J, Chen K, Huang J, Lee S, Wang J, Gao J, et al. PET/NIRF/MRI triple functional iron oxide nanoparticles. Biomaterials. 2010 Apr;31(11):3016–22.
- 38. Gaucher G, Marchessault RH, Leroux JC. Polyester-based micelles and nanoparticles for the parenteral delivery of taxanes. Journal of Controlled Release. 2010 Apr 2;143(1):2–12.
- 39. Zielińska A, Carreiró F, Oliveira AM, Neves A, Pires B, Venkatesh DN, et al. Polymeric Nanoparticles: Production, Characterization, Toxicology and Ecotoxicology. Molecules. 2020 Aug 15;25(16):3731.
- 40. Szalay B, Tátrai E, Nyírő G, Vezér T, Dura G. Potential toxic effects of iron oxide nanoparticles in *in vivo* and *in vitro* experiments. J of Applied Toxicology. 2012 Jun;32(6):446–53.
- 41. Rezazadeh M, Safaran R, Minaiyan M, Mostafavi A. Preparation and characterization of Eudragit L 100-55/chitosan enteric nanoparticles containing omeprazole using general factorial design: in vitro/in vivo study. Research in Pharmaceutical Sciences. 2021 Aug;16(4):358–69.
- 42. Hasnath Siddique DrRA. Prevalence of Peptic Ulcer Disease among the Patients with Abdominal Pain Attending the Department Of Medicine in Dhaka Medical College Hospital, Bangladesh. IOSRJDMS. 2014;13(1):05–20.
- 43. Slavov L, Abrashev MV, Merodiiska T, Gelev Ch, Vandenberghe RE, Markova-Deneva I, et al. Raman spectroscopy investigation of magnetite nanoparticles in ferrofluids. Journal of Magnetism and Magnetic Materials. 2010 Jul;322(14):1904–11.
- 44. Sengani M, Grumezescu AM, Rajeswari VD. Recent trends and methodologies in gold nanoparticle synthesis A prospective review on drug delivery aspect. OpenNano. 2017;2:37–46.
- 45. Bhakay A, Azad M, Bilgili E, Dave R. Redispersible fast dissolving nanocomposite microparticles of poorly water-soluble drugs. International Journal of Pharmaceutics. 2014 Jan:461(1–2):367–79.
- 46. Jeevanandam J, Barhoum A, Chan YS, Dufresne A, Danquah MK. Review on nanoparticles and nanostructured materials: history, sources, toxicity and regulations. Beilstein J Nanotechnol. 2018 Apr 3;9:1050–74.
- 47. Barbosa DB, Monteiro DR, Takamyia AS, Camargo ER, Agostinho AM, Delbem ACB, et al. Silver and Phosphate Nanoparticles. In: Nanobiomaterials in Clinical Dentistry [Internet]. Elsevier; 2013 [cited 2025 Feb 6]. p. 187–202. Available from: https://linkinghub.elsevier.com/retrieve/pii/B978145573127500009X
- 48. Ballauff M, Lu Y. "Smart" nanoparticles: Preparation, characterization and applications. Polymer. 2007 Mar;48(7):1815–23.
- 49. Basso J, Mendes M, Silva J, Cova T, Luque-Michel E, Jorge AF, et al. Sorting hidden patterns in nanoparticle performance for glioblastoma using machine learning algorithms. International Journal of Pharmaceutics. 2021 Jan;592:120095.
- 50. Tiwari AD, Mishra AK, Mishra SB, Kuvarega AT, Mamba BB. Stabilisation of silver and copper nanoparticles in a chemically modified chitosan matrix. Carbohydrate Polymers. 2013 Feb;92(2):1402–7.
- 51. Guardia P, Batlle-Brugal B, Roca AG, Iglesias O, Morales MP, Serna CJ, et al. Surfactant effects in magnetite nanoparticles of controlled size. Journal of Magnetism and Magnetic Materials. 2007 Sep;316(2):e756–9.
- 52. Yoon KY, Hoon Byeon J, Park JH, Hwang J. Susceptibility constants of Escherichia coli and Bacillus subtilis to silver and copper nanoparticles. Science of The Total Environment. 2007 Feb;373(2–3):572–5.



- 53. Kang Y, Huang Y, Yang R, Zhang C. Synthesis and properties of core–shell structured Fe(CO)5/SiO2 composites. Journal of Magnetism and Magnetic Materials. 2016 Feb;399:149–54.
- 54. Sathiyanarayanan G, Seghal Kiran G, Selvin J. Synthesis of silver nanoparticles by polysaccharide bioflocculant produced from marine Bacillus subtilis MSBN17. Colloids and Surfaces B: Biointerfaces. 2013 Feb;102:13–20.
- 55. Yang H, Shi R, Zhang K, Hu Y, Tang A, Li X. Synthesis of WO3/TiO2 nanocomposites via sol–gel method. Journal of Alloys and Compounds. 2005 Aug;398(1–2):200–2.
- 56. Heiligtag FJ, Niederberger M. The fascinating world of nanoparticle research. Materials Today. 2013 Jul;16(7–8):262–71.
- 57. Power A. The Preparation and Characterisation of Silver Nanomaterials and Their Application in Sensing Techniques. 2011 [cited 2025 Feb 6]; Available from: http://arrow.dit.ie/sciendoc/127/
- 58. Bessa PC, Machado R, Nürnberger S, Dopler D, Banerjee A, Cunha AM, et al. Thermoresponsive self-assembled elastin-based nanoparticles for delivery of BMPs. Journal of Controlled Release. 2010 Mar;142(3):312–8.
- 59. J. V Dz and U. Bogdanovic, "Anisotropic silver nanoparticles as filler for the formation of hybrid nanocomposites aponjic," Mater. Res. Bull., vol. 48, pp. 52–57, 2013, doi: 10.1016/j.materresbull.2012.09.059.
- 60. A. Bhakay, M. Azad, E. Bilgili, and R. Dave, "Redispersible fast dissolving nanocomposite microparticles of poorly water-soluble drugs," Int. J. Pharm., vol. 461, no. 1–2, pp. 367–379, 2014, doi: 10.1016/j.ijpharm.2013.11.059.
- 61. P. Chaubey and B. Mishra, "Mannose-conjugated chitosan nanoparticles loaded with rifampicin for the treatment of visceral leishmaniasis," Carbohydr. Polym., vol. 101, no. 1, pp. 1101–1108, 2014, doi: 10.1016/j.carbpol.2013.10.044.
- 62. X. Sheng., "Formation Of Copper And Nickel Nanoparticles By Through In Partial Fulfillment Of The Requirements For Formation Of Copper And Nickel Nanoparticles By," 2012.
- 63. M. Yadi et al., "Current developments in green synthesis of metallic nanoparticles using plant extracts: a review," Artif. Cells, Nanomedicine Biotechnol., vol. 46, no. sup3, pp. \$336–\$343, 2018, doi: 10.1080/21691401.2018.1492931.
- 64. W. Zeng et al., "Hydrothermal synthesis, characterization of h-WO3 nanowires and the gas sensing of thin film sensor based on this powder," Thin Solid Films, pp. 1–20, 2014, doi: 10.1016/j.tsf.2014.12.037.
- 65. A. Costa, B. Sarmento, and V. Seabra, "Mannose-functionalized solid lipid nanoparticles are e ff ective in targeting alveolar macrophages," Eur. J. Pharm. Sci., vol. 114, no. December 2017, pp. 103–113, 2018, doi: 10.1016/j.ejps.2017.12.006.
- 66. G. Gaucher, R. H. Marchessault, and J. Leroux, "Polyester-based micelles and nanoparticles for the parenteral delivery of taxanes," J. Control. Release, vol. 143, no. 1, pp. 2–12, 2010, doi: 10.1016/j.jconrel.2009.11.012.
